

Stability Analysis of Decentralized PVFC Algorithm for Cooperative Mobile Robotic Systems

Jin-Ho Suh*, and Kwon Soon Lee**

* Department of Electrical Engineering, Dong-A University, Busan, Korea
(Tel : +82-51-200-6950; E-mail: suhgang@hanmail.net)

** Division of Electrical, Electronics, and Computer Engineering, Dong-A University, Busan, Korea
(Tel : +81-51-200-7739; E-mail: kwlee@daunet.donga.ac.kr)

Abstract: Passive velocity field control (PVFC) was previously developed for fully mechanical systems, in which the motion task was specified behaviorally in terms of a velocity field, and the closed-loop was passive with respect to a supply rate given by the environment input. However the PVFC was only applied to a single manipulator, the proposed control law was derived geometrically, and the geometric and robustness properties of the closed-loop system were also analyzed. In this paper, we propose a method to apply a decentralized control algorithm to cooperative 3-wheeled mobile robots whose subsystem is under nonholonomic constraints and which convey a common rigid object in a horizontal plain. Moreover it is shown that multiple robot systems ensure stability and the velocities of augmented systems convergence to a scaled multiple of each desired velocity field for cooperative mobile robot systems.

Keywords: Decentralized control, Passive velocity field control(PVFC), Passivity, Mobile robot, Virtual flywheel system

1. INTRODUCTION

The traditional manipulation task is specified by means of a desired timed trajectory in the workspace, which the manipulator is required to track at every instant of time. However, there are many tasks in which the desired motions are specified by the state of system rather than time, such as contour following tasks, painting so on in which target point of the system should keep a contact with an environment. Indeed, it has been demonstrated in many researches^{[3][4]} that in the presence of uncertainties, trajectory based contour tracking algorithms tend to exhibit the radial reduction phenomenon where the radius of the actual contour is smaller than the desired one. Moreover if the desired trajectory was specified in terms of time and rigid servo controller was implemented, the big forces would give damage to the system due to the tracking error. To encode a contour following task, the velocity field should have the following properties:

- (1) Its value at each point of the contour must be tangent to the contour
- (2) The flow of the field has a limit set which is contained in the contour

Based on the considerations, passive velocity field control (PVFC) had been proposed by Li and the geometry of the controlled systems is analyzed.^[3] The methodology encoded tasks using time invariant desired velocity fields instead of the more traditional method. To these ends, the formulation of PVFC has two distinct features as follows:

- (1) The task is encoded desired behavior of the mechanical system is specified in terms of velocity fields defined on the configuration manifold of the system.
- (2) The mechanical system under closed-loop control appears to be an energetically passive system to its physical environments.

Note that the mechanical system is not required to be at a particular position at each time. Instead, the velocity field guides the robot to approach the contour in a well behaved manner. Moreover, the motivations for developing PVFC were to tackle robotic applications that require *i) intimate interaction between the machine and uncertain physical environments* and *ii) the coordination between the various degrees of freedom of the machine for the task to be accomplished*. The block diagram of PVFC can be shown in

Fig. 1 and the key passivity and convergence properties of PVFC were summarized by Li.^[3]

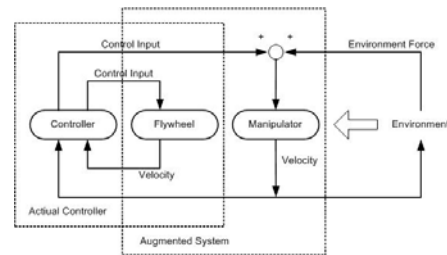


Fig. 1 Passive velocity field control

However the PVFC algorithm applied to a single manipulator could not extend to multiple robot systems. Multiple robotic systems in coordination can execute various tasks which could not be done by a single manipulator such as the handling of a heavy object, etc. Moreover many control algorithms of robot systems have been proposed for the coordinated motion control of multiple robot systems. Therefore typical algorithms for multiple robot systems may be *i) centralized control algorithm* and *ii) decentralized control algorithm*. Especially, to overcome the problems of centralized control algorithm, several decentralized control algorithms have been proposed, in which each robot system is controlled by its own controller without explicit communication among the cooperative systems.

In our pervious research^[4], the decentralized implementation of PVFC including internal force control was proposed in a case where an object is grasped rigidly by multiple manipulators. In this paper, we propose a method to apply an original PVFC with some modification to cooperative mobile robotic systems which consist of two planar mobile robots which convey a common rigid object attached to the mobile robots with passive rotational joints in a horizontal plain. Each mobile robot is a 3-wheeled mobile robot and is under nonholonomic constraints. The specifications of proposed controller are as follows:

- (1) The center of the object follows a desired velocity field without external disturbances.
- (2) The orientation of the object tracks a desired value specified in terms of the position of center of an

object.

(3) Linear motion of an object has properties of a system controlled by an original PVFC.

(4) Internal force is controlled in a certain direction.

Moreover it is shown that multiple robot systems ensure stability and the velocities of augmented systems convergence to a scaled multiple of each desired velocity field for cooperative mobile robot systems. In this paper, we will focus on how to realize the specification above by decentralized PVFC controller through a centralized PVFC.

2. WHEELED MOBILE ROBOTS

We consider a 3-wheeled mobile robot with two conventional fixed wheels on the same axle and one conventional off-centered orientable wheel as shown in Fig. 2. The two conventional fixed wheels (① and ②) have a fixed orientation while the orientation of wheel ③ is varying.

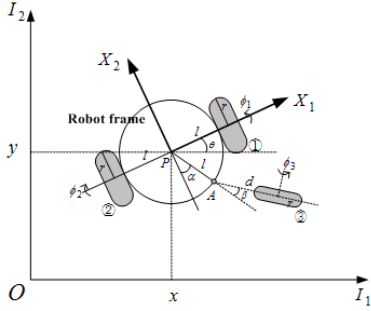


Fig. 2 Configuration of a 3-wheeled mobile robot

According to these descriptions, the geometry of the wheels is completely described by the following class;

$$\{r, l, d, \alpha_i, \beta_i, \phi_i; i = 1, 2, 3\} \quad (1)$$

In Fig. 2, the motion of body of mobile robot is completely specified in terms of the position of reference point P , the position of robot (x, y) , and the rotation of body θ . Therefore we know the vector ξ to indicate the motion of robot body:

$$\xi = (x \ y \ \theta)^T \quad (2)$$

Furthermore, we can introduce the generalized coordinate vector to describe the whole motion of robot in Fig. 2 as follows:

$$q(t) = (x \ y \ \theta \ \beta \ \phi_1 \ \phi_2 \ \phi_3)^T \quad (3)$$

Using the generalized coordinate vector in eq.(3) and the kinematical constraints by the following constraints; i) *pure rolling condition* and ii) *non-slipping condition*, we can also represented the dynamic equation of a 3-wheeled mobile robot by

$$H(\beta)\dot{\zeta}(t) + f(\beta, \zeta) = G(\beta)\tau_m \quad (4)$$

And it is easily shown that these constraints are nonholonomic constraints for the system since two vector fields which satisfy the conditions are not involutive.

If we assume some conditions and use the following coordinate change

$$\begin{aligned} \zeta_1 &= -\dot{x}\sin\theta + \dot{y}\cos\theta \\ \zeta_2 &= \dot{\theta} \end{aligned} \quad (5)$$

and input transformation, we can obtain the simplified dynamic equation as follows:

$$\begin{pmatrix} \dot{\phi} \\ \dot{\theta} \\ \dot{x} \\ \dot{y} \\ \dot{\beta} \\ \dot{\zeta}_1 \\ \dot{\zeta}_2 \end{pmatrix} = \begin{pmatrix} \zeta_1 \\ \zeta_2 \\ -\zeta_1 \sin\theta \\ \zeta_1 \cos\theta \\ -\frac{1}{d}\zeta_1 \sin\beta - \frac{1}{d}\zeta_2(d + l \cos\beta) \\ v_1 \\ v_2 \end{pmatrix} \quad (6)$$

where $v = (v_1 \ v_2)^T$ is a new input, and the constraints are also represented by

$$\begin{aligned} \dot{x}\cos\theta + \dot{y}\sin\theta &= 0 \\ -\dot{x}\sin\theta + \dot{y}\cos\theta &= \zeta_1 \end{aligned} \quad (7)$$

3. MULTIPLE WHEELED MOBILE ROBOTS

3.1 Cooperative 3-wheeled mobile robots

In this paper, the configuration of cooperative 3-wheeled mobile robots are shown in Fig. 3. In considered robot systems, an object denoted by a rod is connected to each mobile robot by a free joint without friction and the length of an object is $2L$.

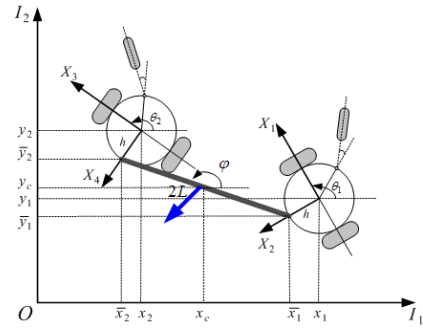


Fig. 3 Configuration of cooperative 3-wheeled mobile robots

If we assume that mass and inertia of an object are m and I_o , and a position of the mass center and rotational angle of an object from $O-I_1$ in counterclockwise direction are (x_c, y_c) and ϕ , then we have free dynamic equations of an object as follows:

$$M_o \ddot{x}_o = 0 \quad (2)$$

$$I_o \ddot{\phi} = 0 \quad (3)$$

where

$$M_o = \begin{pmatrix} m & 0 \\ 0 & m \end{pmatrix}, \quad x_o = (x_c \ y_c)^T \quad (4)$$

On the other hand, since the dynamic equation for two 3-wheeled mobile robots can be described by the previous section which described the modeling of 3-wheeled mobile robot, an augmented dynamic equation is represented as follows:

$$\begin{pmatrix} H_1(\beta_1) & 0 \\ 0 & H_2(\beta_2) \end{pmatrix} \begin{pmatrix} \dot{\eta}_1(t) \\ \dot{\eta}_2(t) \end{pmatrix} + \begin{pmatrix} f_1(\beta_1, \eta_1) \\ f_2(\beta_2, \eta_2) \end{pmatrix} = \begin{pmatrix} G_1(\beta_1) & 0 \\ 0 & G_2(\beta_2) \end{pmatrix} \begin{pmatrix} \tau_{m1} \\ \tau_{m2} \end{pmatrix} \quad (5)$$

for simplicity,

$$H^*(\beta)\dot{\eta}(t) + F^*(\beta, \eta) = G^*(\beta)u(t). \quad (6)$$

where

$$u(t) = (\tau_{m1} \ \tau_{m2})^T, \ \eta(t) := (\eta_1 \ \eta_2)^T, \ \eta_1(t) = (\zeta_1 \ \zeta_2)^T, \\ \eta_2(t) = (\zeta_3 \ \zeta_4)^T, \text{ and } \zeta_i(t) \in \mathfrak{R}, (i=1,2,3,4).$$

That is, each subscript number indicates a number of mobile robot except for ζ_i . As ζ_i disappear alone in the following, we note that there should be no confusion.

On the other hand, using the dynamic equations of an object and each mobile robot, the whole dynamic system without constraint introduced by passive joints can be represented as follows:

$$\begin{pmatrix} H^*(\beta) & 0_{1 \times 2} & 0 \\ 0_{1 \times 4} & M_o & 0 \\ 0_{1 \times 4} & 0_{1 \times 2} & I_o \end{pmatrix} \begin{pmatrix} \dot{\eta}(t) \\ \ddot{x}_o(t) \\ \ddot{\varphi}(t) \end{pmatrix} + \begin{pmatrix} F^*(\beta, \eta) \\ 0 \\ 0 \end{pmatrix} = \begin{pmatrix} G^* \\ 0 \\ 0 \end{pmatrix} u(t). \quad (7)$$

This equation is also rewritten by

$$M_w \ddot{x}_w + F_w = G_w u, \quad (8)$$

where the above term are

$$M_w = \begin{pmatrix} H^*(\beta) & 0_{1 \times 2} & 0 \\ 0_{1 \times 4} & M_o & 0 \\ 0_{1 \times 4} & 0_{1 \times 2} & I_o \end{pmatrix}, \ F_w = \begin{pmatrix} F^*(\beta, \eta) \\ 0 \\ 0 \end{pmatrix}, \ G_w = \begin{pmatrix} G^* \\ 0 \\ 0 \end{pmatrix}$$

$$\dot{x}_w = (\eta(t) \ \dot{x}_o(t) \ \dot{\varphi}(t))^T, \ \eta(t) = (\eta_1(t) \ \eta_2(t))^T.$$

From the kinematic constraints by the passive joints, the holonomic constraints between the generalized coordinates are defined by

$$\begin{pmatrix} \bar{x}_1 \\ \bar{y}_1 \end{pmatrix} = \begin{pmatrix} x_1 - h \sin \theta_1 \\ y_1 + h \cos \theta_1 \end{pmatrix} = \begin{pmatrix} x_c - L \cos \varphi \\ y_c + L \sin \varphi \end{pmatrix} \quad (9)$$

$$\begin{pmatrix} \bar{x}_2 \\ \bar{y}_2 \end{pmatrix} = \begin{pmatrix} x_2 - h \sin \theta_2 \\ y_2 + h \cos \theta_2 \end{pmatrix} = \begin{pmatrix} x_c + L \cos \varphi \\ y_c - L \sin \varphi \end{pmatrix} \quad (10)$$

Using the differential of eq. (9) and eq. (10), and the definition of $\eta_i(t), (i=1,2)$, we can represent above equations as matrix form as follows:

$$\underbrace{\begin{pmatrix} J_1 & 0_{2 \times 2} & & \\ & & J_o & J_\varphi \\ 0_{2 \times 2} & J_2 & & \end{pmatrix}}_{:=J_w} \begin{pmatrix} \eta_1(t) \\ \eta_2(t) \\ \dot{x}_o \\ \dot{\varphi} \end{pmatrix} = \begin{pmatrix} 0_{2 \times 1} \\ 0_{2 \times 1} \\ 0_{2 \times 1} \\ 0 \end{pmatrix} \quad (11)$$

for simplicity,

$$J_w \dot{x}_w = 0 \quad (12)$$

where

$$J_i = \begin{pmatrix} -\sin \theta_i & -h \cos \theta_i \\ \cos \theta_i & -h \sin \theta_i \end{pmatrix}, \ (i=1,2) \quad (13)$$

$$J_o = (-I_{2 \times 2} \ -I_{2 \times 2})^T \quad (14)$$

$$J_\varphi = (-L \sin \varphi \ -L \cos \varphi \ L \sin \varphi \ L \cos \varphi)^T \quad (15)$$

$$x_w = (\eta_1 \ \eta_2 \ \dot{x}_o \ \dot{\varphi})^T \quad (16)$$

Therefore the actual dynamic equation for whole can be represented as follows:

$$M_w \ddot{x}_w + F_w = G_w u - J_w^T \lambda \quad (17)$$

where $\lambda \in \mathfrak{R}^4$ is a constraint force vector and it is also defined by

$$\lambda = (\lambda_1 \ \lambda_2)^T, \ \lambda_1 = (\lambda_{m1} \ \lambda_{m2})^T, \ \lambda_2 = (\lambda_{m3} \ \lambda_{m4})^T \quad (18)$$

If we define the constraint force as above equations, eq. (18), the actual dynamic equation of whole system can be decomposed into the following equations using eq. (17):

$$H_i(\beta_i) \dot{\eta}(t) + f_i(\beta_i, \eta_i) = G_i(\beta_i) \tau_{mi} - J_i^T \lambda_i \quad (i=1,2) \quad (19)$$

$$M_o \ddot{x}_o = -J_o^T \lambda \quad (20)$$

$$I_o \ddot{\varphi} = -J_\varphi^T \lambda \quad (21)$$

3.2 Minor loop compensation

Since we assume that the constraint forces, $\lambda_i (i=1,2)$ are observed by each force sensor in our control method, then we can define a local control input, $\tau_{mi} (i=1,2)$ given by

$$\tau_{mi} = G_i^{-1}(H_i v_i + f_i + J_i^T \lambda_i) - G_i^{-1} H_i J_i^T \lambda_i \quad (i=1,2) \quad (22)$$

where $v_i (i=1,2)$ is new input and it will also describe in the next. If we inject new control input v_i into cooperative 3-wheeled mobile robot systems, then we can define the closed loop system substituting eq. (20) into eq. (21)

$$\dot{\eta}_i(t) = v_i(t) - J_i^T \lambda_i \quad (i=1,2) \quad (23)$$

Recomposing eq. (20), eq. (21), and eq. (23), the actual dynamic equation of whole system is described by the matrix form of the given equations

$$\bar{M}_w \ddot{x}_w = \bar{G}_w v(t) - J_w^T \lambda \quad (24)$$

where

$$\bar{M}_w = \begin{pmatrix} I_{2 \times 2} & & & \\ & I_{2 \times 2} & & \\ & & M_o & \\ & & & I_o \end{pmatrix}, \ \bar{G}_w = \begin{pmatrix} I_{2 \times 2} & & 0_{2 \times 2} \\ 0_{2 \times 2} & & I_{2 \times 2} \\ & 0_{2 \times 4} & \\ & & 0_{1 \times 4} \end{pmatrix} \quad (25)$$

$$v = (v_1 \ v_2 \ 0_{2 \times 1} \ 0)^T \quad (26)$$

We note that the minor loop compensation is not necessary for the design of passive velocity field control, but the computation for the passive velocity field control would become very complex.

Since the motions of x_o and φ should be controlled in our control problem and the direct control input for φ does not exist, the distributed control method proposed in our previous research^[4] can not be applied for this paper directly. The dynamic equation is transformed by a coordinate transformation and input change in advance so that the dynamic system of φ disappear in the equation. Therefore the control input for φ is realized as an internal force for the motion of x_o .

Let's define $\dot{\bar{x}}_i$ as follows:

$$\dot{\bar{x}}_i = J_i \eta_i(t) \quad (i=1,2) \quad (27)$$

Then, using the new coordinate $\dot{\bar{x}}_i$, the actual dynamic equation of 3-wheeled mobile robots given by eq. (24) can be rewritten by the following equations

$$J_i^{-1} \ddot{\bar{x}}_i - J_i^{-1} \dot{J}_i J_i^{-1} \dot{\bar{x}}_i = v_i - J_i^T \lambda_i \quad (i=1,2) \quad (28)$$

Therefore the actual dynamic equation of whole system given by eq. (20), eq. (21), and eq. (28) can be represented by matrix form as follows:

$$\begin{pmatrix} J_1^{-1} & & & \\ & J_2^{-1} & & \\ & & M_o & \\ & & & I_o \end{pmatrix} \begin{pmatrix} \ddot{\bar{x}}_1 \\ \ddot{\bar{x}}_2 \\ \ddot{x}_o \\ \ddot{\varphi} \end{pmatrix} + \begin{pmatrix} -J_1^{-1} \dot{J}_1 J_1^{-1} \dot{\bar{x}}_1 \\ -J_2^{-1} \dot{J}_2 J_2^{-1} \dot{\bar{x}}_2 \\ 0_{2 \times 1} \\ 0 \end{pmatrix}$$

$$= \begin{pmatrix} v_1 \\ v_2 \\ \mathbf{0}_{2 \times 1} \\ 0 \end{pmatrix} - \begin{pmatrix} J_1^T & \mathbf{0}_{2 \times 2} \\ \mathbf{0}_{2 \times 2} & J_2^T \\ J_o^T & \\ J_\varphi^T & \end{pmatrix} \begin{pmatrix} \lambda_{m1} \\ \lambda_{m2} \\ \lambda_{m3} \\ \lambda_{m4} \end{pmatrix} \quad (29)$$

Substituting $\dot{\bar{x}}_i$ defined by eq. (27) into eq. (12), we also obtain the following results

$$J_w \begin{pmatrix} J_1^{-1} & & & \\ & J_2^{-1} & & \\ & & I_{2 \times 2} & \\ & & & 1 \end{pmatrix} \begin{pmatrix} \dot{\bar{x}}_1 \\ \dot{\bar{x}}_2 \\ \dot{x}_o \\ \dot{\varphi} \end{pmatrix} = \begin{pmatrix} \mathbf{0}_{2 \times 1} \\ \mathbf{0}_{2 \times 1} \\ \mathbf{0}_{2 \times 1} \\ 0 \end{pmatrix} \quad (30)$$

To represent the actual dynamic equation of whole system newly, we first define the matrix \bar{J}_w as follows:

$$\bar{J}_w := \begin{pmatrix} J_1^{-T} & & & \\ & J_2^{-T} & & \\ & & I_{2 \times 2} & \\ & & & 1 \end{pmatrix} \quad (31)$$

At this time, pre-multiplying a matrix defined by eq. (31) in eq. (29), we can describe new dynamic equation of whole system as follows:

$$\begin{pmatrix} J_1^{-T} J_1^{-1} & & & \\ & J_2^{-T} J_2^{-1} & & \\ & & M_o & \\ & & & I_o \end{pmatrix} \begin{pmatrix} \ddot{\bar{x}}_1 \\ \ddot{\bar{x}}_2 \\ \ddot{x}_o \\ \ddot{\varphi} \end{pmatrix} + \begin{pmatrix} -J_1^{-T} J_1^{-1} \dot{J}_1 J_1^{-1} \dot{\bar{x}}_1 \\ -J_2^{-T} J_2^{-1} \dot{J}_2 J_2^{-1} \dot{\bar{x}}_2 \\ 0 \\ 0 \end{pmatrix} = \begin{pmatrix} J_1^{-T} v_1 \\ J_2^{-T} v_2 \\ 0 \\ 0 \end{pmatrix} - \underbrace{\begin{pmatrix} I_{2 \times 2} & & & \\ & I_{2 \times 2} & & \\ & & -I_{2 \times 2} & \\ & & & -I_{2 \times 2} \end{pmatrix}}_{:=J_c^T} \begin{pmatrix} \lambda_{m1} \\ \lambda_{m2} \\ \lambda_{m3} \\ \lambda_{m4} \end{pmatrix} \quad (32)$$

Moreover, using the generalized coordinates in eq. (11), J_c^T to eq. (32) is also derived by

$$J_c \dot{\bar{x}}_w = 0 \quad (33)$$

where

$$\bar{x}_w = (\bar{x}_1 \quad \bar{x}_2 \quad x_o \quad \varphi)^T \quad (34)$$

Furthermore, if we define new input $v_i(t)$ in eq. (22) as

$$v_i(t) = J_i^{-1}(v_i - \dot{J}_i J_i^{-1} \dot{\bar{x}}_i) + (J_i^T - J_i^{-1}) \lambda_i \quad (i=1, 2) \quad (35)$$

then the dynamic equation of whole system, eq. (29), which is represented by new coordinate, \bar{x}_i is simply described by

$$\begin{pmatrix} I_{2 \times 2} & & & \\ & I_{2 \times 2} & & \\ & & M_o & \\ & & & I_o \end{pmatrix} \begin{pmatrix} \ddot{\bar{x}}_1 \\ \ddot{\bar{x}}_2 \\ \ddot{x}_o \\ \ddot{\varphi} \end{pmatrix} = \begin{pmatrix} v_1 \\ v_2 \\ \mathbf{0}_{2 \times 1} \\ 0 \end{pmatrix} - \begin{pmatrix} I_{2 \times 2} & & & \\ & I_{2 \times 2} & & \\ & & -I_{2 \times 2} & \\ & & & -I_{2 \times 2} \end{pmatrix} \begin{pmatrix} \lambda_{m1} \\ \lambda_{m2} \\ \lambda_{m3} \\ \lambda_{m4} \end{pmatrix} \quad (36)$$

where v_i ($i=1, 2$) is an actual control input. Finally, the dynamic equations in eq. (33) and eq. (36) can be represented as follows:

$$\bar{M}_w \ddot{\bar{x}}_w = (v_1 \quad v_2 \quad \mathbf{0}_{2 \times 1} \quad 0)^T - J_c^T \lambda \quad (37)$$

$$J_c \dot{\bar{x}}_w = 0 \quad (38)$$

Using the generalized coordinate to eq. (9) - eq. (10) and the differentiation of these equations, we can derive the following equations from the relationship between the position of mass center $x_o = (x_c \quad y_c)^T$ and new coordinate \bar{x}_i ($i=1, 2$) as follows:

$$\begin{pmatrix} \dot{x}_c \\ \dot{y}_c \end{pmatrix} = \underbrace{\begin{pmatrix} -\sin \theta_1 & -h \cos \theta_1 \\ \cos \theta_1 & -h \sin \theta_1 \end{pmatrix}}_{:=J_1 \eta_1 = \dot{\bar{x}}_1} \begin{pmatrix} \zeta_1 \\ \zeta_2 \end{pmatrix} + \underbrace{\begin{pmatrix} -L \sin \varphi \\ -L \cos \varphi \end{pmatrix}}_{:= (I_{2 \times 2} \quad \mathbf{0}_{2 \times 2}) J_\varphi} \dot{\varphi} \quad (39)$$

$$\begin{pmatrix} \dot{x}_c \\ \dot{y}_c \end{pmatrix} = \underbrace{\begin{pmatrix} -\sin \theta_2 & -h \cos \theta_2 \\ \cos \theta_2 & -h \sin \theta_2 \end{pmatrix}}_{:=J_2 \eta_2 = \dot{\bar{x}}_2} \begin{pmatrix} \zeta_3 \\ \zeta_4 \end{pmatrix} + \underbrace{\begin{pmatrix} L \sin \varphi \\ L \cos \varphi \end{pmatrix}}_{:= (\mathbf{0}_{2 \times 2} \quad I_{2 \times 2}) J_\varphi} \dot{\varphi} \quad (40)$$

for simplicity,

$$\dot{x}_o = \dot{\bar{x}}_1 + (I_{2 \times 2} \quad \mathbf{0}_{2 \times 2}) J_\varphi \dot{\varphi} \quad (41)$$

$$\dot{x}_o = \dot{\bar{x}}_2 + (\mathbf{0}_{2 \times 2} \quad I_{2 \times 2}) J_\varphi \dot{\varphi} \quad (42)$$

Furthermore, substituting the differentiations of eq. (41) and eq. (42) into eq. (37), we can also describe as follows:

$$\ddot{x}_o - (I_{2 \times 2} \quad \mathbf{0}_{2 \times 2}) (J_\varphi \ddot{\varphi} + \dot{J}_\varphi \dot{\varphi}) = v_1 - \lambda_1 \quad (43)$$

$$\ddot{x}_o - (\mathbf{0}_{2 \times 2} \quad I_{2 \times 2}) (J_\varphi \ddot{\varphi} + \dot{J}_\varphi \dot{\varphi}) = v_2 - \lambda_2 \quad (44)$$

4. DECENTRALIZED CONTROLLER DESIGN

In order to design the decentralized PVFC, we assume that $\ddot{\varphi}$ is measurable for each subsystem in this paper, which is a crucial step to derive the decentralized PVFC since $\ddot{\varphi}$ is determined based on both λ_1 and λ_2 , and both signals can not be used for each subsystem in the decentralized formulation. That is, it means that λ_1 can be used only in the subsystem 1 so on.

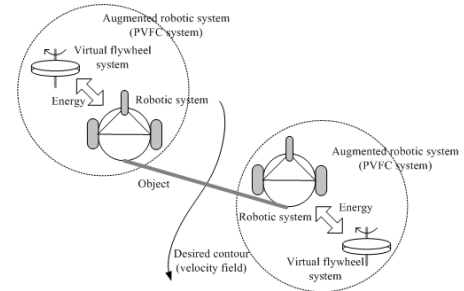


Fig. 4 Conception of decentralized PVFC scheme

The effectiveness of this assumption will be demonstrated in the simulation and experimental results, respectively. Furthermore, the decentralized PVFC scheme in this paper is shown in Fig. 4.

4.1 Augmented mechanical system

If the actual control input is defined as

$$v_1 = v'_1 - (I_{2 \times 2} \quad \mathbf{0}_{2 \times 2}) (J_\varphi \ddot{\varphi} + \dot{J}_\varphi \dot{\varphi}) \quad (45)$$

$$v_2 = v'_2 - (\mathbf{0}_{2 \times 2} \quad I_{2 \times 2}) (J_\varphi \ddot{\varphi} + \dot{J}_\varphi \dot{\varphi}) \quad (46)$$

Then we can rewrite eq. (43) and eq. (44) as follows:

$$\ddot{x}_o = v'_i - \lambda_i \quad (i=1, 2) \quad (47)$$

Adding the dynamic equation of x_o in eq. (36) and eq. (47), we can describe the motion equation of an object as follows:

$$(I_{2 \times 2} + M_o + I_{2 \times 2}) \ddot{x}_o = v'_1 + v'_2 \quad (48)$$

In eq. (48), it can be seen that the dynamic equation of mass center x_o is the same as that of connected three masses, $I_{2 \times 2}$, M_o , and $I_{2 \times 2}$, and the separated masses are controlled by v'_1 and v'_2 , respectively.

Therefore we can apply a decentralized PVFC proposed in our previous researches to design v'_i ($i=1, 2$).^{[4][5]}

First of all, the procedure in order to apply an individual PVFC algorithm can be designed that the motion equation in eq. (48) is separated as the following virtual dynamic equation

$$(I_{2 \times 2} + \rho_1 M_o) \ddot{x}_o = v'_1 \quad (49)$$

$$(I_{2 \times 2} + \rho_2 M_o) \ddot{x}_o = v'_2 \quad (50)$$

for simplicity,

$$\bar{M}'_i \ddot{x}_o = v'_i \quad (i=1, 2) \quad (51)$$

where ρ_i ($i=1, 2$) is load sharing coefficient and it is satisfied with $\rho_1 + \rho_2 = 1$.

The dynamics of the virtual flywheel is given by

$$M_{fwi} \ddot{x}_{fwi} = v_{fwi} \quad (i=1, 2) \quad (52)$$

where v_{fwi} ($i=1, 2$) is the coupling control input to the flywheel, which will be defined later on. Thus, the dynamics of the augmented system are composed as follows:

$$\bar{M}'_{ai} \ddot{X}_{ai} = v'_{ai} \quad (i=1, 2) \quad (53)$$

where $\dot{X}_{ai} = (\dot{x}_o \quad \dot{x}_{fwi})^T$ is the velocity of the augmented system, v'_{ai} is the augmented control input, and \bar{M}'_{ai} is the augmented inertia matrix and is defined by

$$\bar{M}'_{ai} = \begin{pmatrix} \bar{M}'_i & 0 \\ 0 & M_{fwi} \end{pmatrix} \quad (54)$$

For each augmented configuration X_{ai} , we define the kinetic energy of the augmented dynamic system \bar{H}'_a which is expressed in local coordinate by

$$\bar{H}'_a = \sum_{i=1}^2 \frac{1}{2} \dot{X}_{ai}^T \bar{M}'_{ai} \dot{X}_{ai} \quad (55)$$

4.2 Generation of augmented desired velocity field

For the augmented mechanical system, an augmented desired velocity field V_{ai} is needed. It is defined so that the following condition is satisfied:^[3]

Condition 1: The augmented desired velocity field V_{ai} satisfies:

Conservation of kinetic energy: The total kinetic energy of the augmented system evaluated at the desired velocity field is constant, i.e., the following condition is satisfied for all X_{ai} :

$$\bar{H}'_{ai} = \sum_{i=1}^2 \frac{1}{2} \dot{X}_{ai}^T \bar{M}'_{ai} \dot{X}_{ai} = \bar{E}_i > 0 \quad (56)$$

where \bar{E}_i is a positive constant.

Consistency: The component of the augmented velocity field that corresponds to the original dynamic equation of motion system should be the same as the specified desired velocity field, i.e., V_{ai} is of the form

$$V_{ai} = (V_i \quad V_{n+1})^T \quad (57)$$

Also, it is satisfied as follows:

$$V_{n+1} = \sqrt{\frac{2}{M_{fwi}} (\bar{E}_i - \frac{1}{2} V_i \bar{M}'_i V_i)} \quad (58)$$

Notice that \bar{E}_i ($i=1, 2$) should be selected to be large enough so that eq. (58) has a real solution. It should now be apparent that the virtual inertia acts as a reservoir of kinetic energy.^{[3][4]}

4.3 Coupling control law

As expressed by an original PVFC algorithm, the coordinate representations of these objects are

$$\bar{P}_{ai} = \bar{M}'_{ai} \dot{X}_{ai}, \quad \bar{Q}_{ai} = \bar{M}'_{ai} V_{ai}, \quad \bar{\Delta}_{ai} = \bar{M}'_{ai} \dot{V}_{ai} \quad (59)$$

where \bar{P}_{ai} , \bar{Q}_{ai} , and $\bar{\Delta}_{ai}$ ($i=1, 2$) are the momentums of the augmented system, the desired momentums of the augmented system, and the momentums of associated with the covariant derivative of the desired velocity field with respect to the actual robot velocities, respectively.

Then the coupling control law in eq. (59) is given by

$$v'_{ai} = (\bar{G}_{ai} + \gamma_i \bar{R}_{ai}) \dot{X}_{ai} \quad (i=1, 2) \quad (60)$$

where

$$\bar{G}_{ai}(X_{ai}, \dot{X}_{ai}) = \frac{1}{2E_i} \underbrace{(\bar{\Delta}_{ai} \bar{Q}_{ai}^T - \bar{Q}_{ai} \bar{\Delta}_{ai}^T)}_{\text{skew symmetric}} \quad (61)$$

$$\bar{R}_{ai} = \underbrace{\bar{Q}_{ai} \bar{P}_{ai}^T - \bar{P}_{ai} \bar{Q}_{ai}^T}_{\text{skew symmetric}} \quad (62)$$

and γ_i ($i=1, 2$) is a control gain, not necessary positive, which determines the convergence rate and the sense in which the desired velocity field will be followed.

For any $\alpha_i \in \mathfrak{R}$, the local coordinate representation of the augmented α_i -velocity error e_{ai} is defined by

$$e_{ai} = \dot{X}_{ai} - \alpha_i V_{ai} \quad (63)$$

Thus, we can obtain the error dynamics for the augmented system in eq. (53) as follows:

$$\bar{M}'_{ai} \dot{e}_{ai} = \bar{G}_{ai} e_{ai} + \gamma_i \bar{R}_{ai} \dot{X}_{ai} \quad (64)$$

Theorem 1: Consider the feedback system for decentralized PVFC as shown in Fig. 5 where the motion equation is given by eq. (51), and the individual PVFC control law consists of the virtual dynamic augmentation eq. (52) and coupling control law eq. (60)–eq. (62). Furthermore if the control input about control internal force is defined by

$$v'_{li} = (1 + k_f) \begin{pmatrix} F_{di} \\ 0 \end{pmatrix} \quad (65)$$

and an actual control input about given system v'_i is also defined by

$$v'_i = v'_{ai} + v'_{li} \quad (i=1, 2) \quad (66)$$

where v'_{li} is desired internal force and satisfies

$$\sum_{i=1}^2 v'_{li} = 0 \quad (67)$$

Then the passivity and convergence properties of decentralized PVFC are summarized as follows:

(1) The augmented feedback system in eq. (53) is passive with respect to the supply rate defined by

$$s(F, \dot{x}) = \langle F, \dot{x} \rangle = F^T \dot{x} \quad (68)$$

where F and \dot{x} are input and output, respectively.

(2) For the augmented α_i -velocity error e_{ai} in eq. (63),

the velocity of an object \dot{X}_{ai} is a Lyapunov stable solution in the absence of environment forces.

Proof of (1): The derivation of kinetic energy defined by eq. (55) satisfies

$$\begin{aligned} \frac{d}{dt} \bar{H}'_{ai} &= \sum_{i=1}^2 (\dot{X}'_{ai} \bar{M}'_{ai} \ddot{X}_{ai} + \frac{1}{2} \dot{X}'_{ai} \bar{M}'_{ai} \dot{X}_{ai}) \\ &= \sum_{i=1}^2 (\dot{X}'_{ai} \bar{M}'_{ai} \ddot{X}_{ai} + \dot{X}_{fwi} \underbrace{M_{fwi} \ddot{X}_{fwi}}_{=V_{fwi}}) + \frac{1}{2} \sum_{i=1}^2 \underbrace{\dot{X}'_{ai} \bar{M}'_{ai} \dot{X}_{ai}}_{=0} \quad (69) \\ &= \sum_{i=1}^2 \dot{X}'_{ai} V'_{ai} = \sum_{i=1}^2 \underbrace{\dot{X}'_{ai} \bar{G}'_{ai} \dot{X}_{ai}}_{=0} + \underbrace{\dot{X}'_{ai} \bar{R}'_{ai} \dot{X}_{ai}}_{=0} = 0 \end{aligned}$$

Therefore, upon integration of eq. (69), we can obtain

$$\int_0^t \dot{\bar{H}}'_{ai}(t) dt = \bar{H}'_{ai}(t) - \bar{H}'_{ai}(0) = 0 > -\bar{H}'_{ai}(0) \quad (70)$$

Since $\bar{H}'_{ai}(0) \geq 0$, the system is passive with respect to the supply rate in eq. (68).

Proof of (2): Given $\alpha \in \mathbb{R}$, let's define the positive definite storage function \bar{W}_α as follows:

$$\bar{W}_\alpha = \frac{1}{2} \sum_{i=1}^2 e_{ai}^T \bar{M}'_{ai} e_{ai} \quad (71)$$

Differentiating eq. (71), utilizing eq. (64) and the fact that $\dot{\bar{M}}'_{ai} + 2\bar{G}'_{ai}$ is skew symmetric, we obtain

$$\begin{aligned} \frac{d}{dt} \bar{W}_\alpha &= \frac{1}{2} \sum_{i=1}^2 (\dot{e}_{ai}^T \bar{M}'_{ai} e_{ai} + \underbrace{e_{ai}^T \dot{\bar{M}}'_{ai} e_{ai}}_{=0} + e_{ai}^T \bar{M}'_{ai} \dot{e}_{ai}) \\ &= \sum_{i=1}^2 \gamma_i (\underbrace{\dot{X}'_{ai} \bar{R}'_{ai} \dot{X}_{ai}}_{=0} - \alpha_i V'_{ai} \bar{R}'_{ai} \dot{X}_{ai}) \quad (72) \\ &= -\sum_{i=1}^2 \alpha_i \gamma_i (4\bar{H}'_{ai} \bar{E}_i - \ll V_{ai}, \dot{X}_{ai} \gg_{ai}^2) \\ &\leq 0 \end{aligned}$$

Since \bar{W}_α is a positive definite function of α_i -velocity error e_{ai} , we know that the augmented α_i -velocity error $e_{ai} = 0$ is Lyapunov stable of the error dynamics using Barlalet's lemma.^{[1][3]} ■

5. SIMULATION RESULTS

This section illustrates the performance of the proposed control algorithm for cooperative 3-wheeled mobile robots using numerical simulations. The considered dynamic models will use the similar ones for experiment and is shown in Fig. 4 based on the constructed experimental system.

Since the desired velocity field is defined such that if a point moves along the desired velocity, the point convergences to a circle whose center and radius are the origin and 1[m] at a constant speed in an anti-clockwise direction. The control is used for both robots and load sharing parameters ρ_i is set to 0.5 since we assumed that each mobile robot has the same capability. For the observation of $\dot{\varphi}$, we will use a minimal order observation which is designed based on triple integrator model where the pole of the observer was chosen to -50.

When we include the external force (10,0)[N] to system from 15[sec] to 20[sec], the simulation results for considered system are shown in Fig. 5-7, respectively.

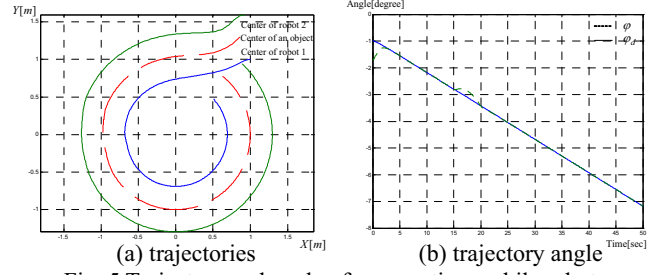


Fig. 5 Trajectory and angle of cooperative mobile robots

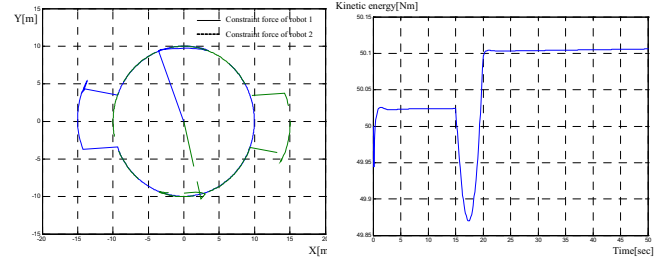


Fig. 6 Constraint forces With disturbance

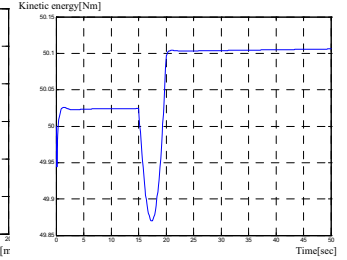


Fig. 7 Kinetic energy of augmented system

6. CONCLUSIONS

In this paper, we propose a new control methodology for cooperative 3-wheeled mobile robotic systems convey a rigid object, and the proposed decentralized control algorithm is analyzed using an original PVFC algorithm. Especially, the closed-loop input/output systems for multiple robotic systems are passive with the environment force as inputs, the system velocities as outputs, and the environment mechanical powers as supply rates as if it is similar to an original PVFC. The closed-loop systems for cooperative mobile robots are very effective in tracking a multiple of each desired velocity field and in counteracting the detrimental effect of environment disturbances when the disturbances are in the directions of the desired momentums of multiple robotic systems.

Moreover, the application of decentralized PVFC algorithm to tracing a circle as well as simulation in order to show effectiveness for the extended PVFC algorithm proposed in this paper.

ACKNOWLEDGMENTS

The work was supported by the National Research Laboratory Program of the Korean Ministry of Science and Technology (MOST).

REFERENCES

- [1] J. J. Slotine and W. Li, *Applied Nonlinear Control*, Prentice-Hall, 1991.
- [2] G. Campion, G. Bastin, and B. D'Andrea-Novet, "Structural Properties and Classification of Kinematic and Dynamic Models of Wheeled Mobile Robots", *IEEE Trans. on Robotics and Automation*, Vol. 12, No. 1, pp. 47-62, 1996.
- [3] P. Y. Li and R. Horowitz, "Passive Velocity Field Control of Mechanical Manipulator", *IEEE Trans. on Robotics and Automation*, Vol. 15, No. 4, pp. 751-763, 1999.
- [4] M. Yamakita, J. H. Suh, and K. Hashiba, "Decentralized PVFC for Cooperative Mobile Robots," *Trans. on IEE Japan*, Vol. 120-C, No. 10, pp. 1485-1491, 2000.
- [5] J. H. Suh, M. Yamakita, and S. B. Kim, "Adaptive Desired Velocity Field Control for Cooperative Mobile Robotic Systems with Decentralized PVFC," *JSME International Journal, Series-C*, Vol. 47, No. 1, pp. 280-288, 2004.